



# Spectral characteristics of a spoke on the Saturn Rings

E. D'Aversa<sup>1</sup>, G. Bellucci<sup>1</sup>, F. Altieri<sup>1</sup>, F.G. Carrozzo<sup>1</sup>, G. Filacchione<sup>2</sup>, F. Tosi<sup>1</sup>,  
P.D. Nicholson<sup>3</sup>, M.M. Hedman<sup>3</sup>, R.H. Brown<sup>4</sup>, and M.R. Showalter<sup>5</sup>

<sup>1</sup> Istituto Nazionale di Astrofisica – Istituto di Fisica dello Spazio Interplanetario, Via Fosso del Cavaliere 100, I-00133 Roma, Italy

e-mail: [emiliano.daversa@ifsi-roma.inaf.it](mailto:emiliano.daversa@ifsi-roma.inaf.it)

<sup>2</sup> Istituto Nazionale di Astrofisica – Istituto di Astrofisica Spaziale e Fisica Cosmica, Via Fosso del Cavaliere 100, I-00133 Roma, Italy

<sup>3</sup> Cornell University, Ithaca, NY, USA

<sup>4</sup> Lunar and Planetary Laboratory, University of Arizona, Tucson, AZ, USA

<sup>5</sup> SETI Institute, Mountain View, CA, USA

**Abstract.** On 2008, July, the Cassini/VIMS spectrometer detected spokes on the Saturn's B ring for the first time. These are the first measurements of the complete reflectance spectrum of spokes in a wide spectral range (0.35-0.51  $\mu\text{m}$ ). Until now, only one spoke, imaged by VIMS on July 9<sup>th</sup>, has been studied in some details. The spectrum is consistent with a population of spheroidal water ice particles with a quite wide size distribution centered at about 1.90  $\mu\text{m}$  (modal radius), i.e. substantially greater than previously thought. This result is obtained, after accurate spatial analyses, by means of radiative transfer modeling of the reflectance spectral contrast of the spoke, making no assumptions about the B ring microphysics. A number density of about 0.01-0.1 grains/cm<sup>3</sup> is also deduced. If confirmed, the unexpected abundance of micron-sized grains may have implications for the spoke physical models, since the amount of energy required for the spoke formation increases by about one order of magnitude. This kind of observations may also constrain the size selection effects thought to be produced by the forces governing the spokes' evolution.

**Key words.** Solar System: Saturn – Rings – Spokes – Water Ice – Infrared spectroscopy

## 1. Introduction

Spokes are broad or elongated markings which occasionally appear on the Saturn's rings, usually across the outer part of the B ring. They have been discovered in Voyager images during the 1980-81 flyby (Smith et al., 1982), then repeatedly detected in a long-

term HST campaign (McGhee et al., 2005), and finally re-observed by the Cassini ISS camera since September 2005 (Mitchell et al., 2006). Several insights about their nature have been deduced from the statistical analysis of available observations, but the process of their formation is not yet fully understood and still debated (e.g., Farmer and Goldreich, 2005; Morfill and Thomas, 2005; Jones et al., 2006). They are known to appear more fre-

---

*Send offprint requests to:* E. D'Aversa

quently near Saturn's equinoxes, in the morning ansa of the rings. They form on a time scale of the order of minutes and fade away in few hours. They are usually located not far from the synchronous orbit radius, where the Keplerian velocity of the ring particles equals the rotation velocity of the Saturn's magnetic field. Anyway the spokes do not follow pure gravitational orbits, since they always appear corotating with the magnetic field. Finally, they are visible at both ring sides, but their reflectance changes substantially with the solar phase angle, since they are darker than the surrounding ring at low phase angles and brighter at high phase angles. These evidences, collected in the last decades, made widely accepted the idea that the spokes are a dusty-plasma phenomenon, caused by the electrostatic levitation of very small ice particles usually deposited on the surface of the boulders which form the ring (Goertz and Morfill, 1983). However, the process which triggers the charging of the boulder surfaces and the subsequent grain levitation is not yet determined. Two main processes have been proposed so far: the micro-meteoritic bombardment on the rings and the lighting from thunderstorms in the Saturn's atmosphere. In both cases, the variation of the plasma environment in which the rings are dipped is invoked to explain the seasonality of the spokes appearance. An increase of incident sunlight, for example, can inhibit the spoke formation since the associated increase in the photoelectrons production negatively charges the plasma near the rings, preventing the levitation. In the case of lighting-induced spokes, further sources of temporal variability are related to the thunderstorm frequency and to the local thickness of the ionosphere.

All the spoke observations available until now were obtained in a limited spectral range. Only six spectral filters were available to the Voyager ISS cameras (between 0.35 and 0.59  $\mu\text{m}$ ). HST/WFPC2 spokes observations used 5 filters between 0.34 and 0.81  $\mu\text{m}$ . Cassini ISS cameras cover about from 0.2 to 1.1  $\mu\text{m}$  in 18 or 24 filters. The images acquired by the Visual and Infrared Mapping Spectrometer (VIMS) on board the Cassini spacecraft are therefore the first spoke observations at wave-

lengths longward of 1.1  $\mu\text{m}$ . The spectra, ranging from 0.35 to 5.1  $\mu\text{m}$  and acquired since July 2008, cover the main water ice absorption bands, making these observations very useful in constraining the spoke grains microphysics (D'Aversa et al., 2010).

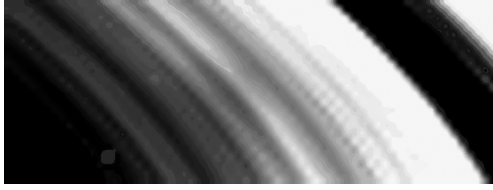
## 2. The VIMS instrument

VIMS is an imaging spectrometer covering the 0.35-5.1  $\mu\text{m}$  spectral range in 352 spectral 32 channels. It is able to produce 64x64 pixels images with two distinct channels (VIMS-V, 0.35-1.05  $\mu\text{m}$ , and VIMS-IR, 0.85-5.1  $\mu\text{m}$ ). We refer to the paper of Brown et al., (2004) for an exhaustive description of the main instrumental issues. Each VIMS spectrum has been accurately georeferenced, by means of specific NAIF-SPICE (Acton, 1996) based algorithms, and calibrated following the standard pipeline (McCord et al., 2004) with the latest available upgrades (2009). The main source of measurement errors for the VIMS spectra of the rings is the spatial resolution, which makes the size of the pixel footprints of the same scale length as the variation of the radiative field.

## 3. The spoke

In this work we illustrate the analysis of a single spoke, observed by VIMS on 2008, July 9<sup>th</sup> (cube 1594203306), shown in Fig. 1 at 2.23  $\mu\text{m}$ . A ring-plane projection of the same image is shown in fig. 2, where the reflectance profiles of the resolved ringlets have been normalized to unity in order to enhance position and shape of the faint spoke. The scene is illuminated 6° over the ring plane, and viewed from 24° elevation with a spatial resolution of about 390 km/pixel in the radial direction and 940 km/pixel in the azimuthal one. The phase angle is 24.5°.

The spoke is roughly elliptical, located about 18° ( $\approx 30$  min) away from the morning Saturn's shadow. It is about 6000 x 2000 km in size, and tilted by about 70° with respect to the radial direction. Keplerian velocity shear would need more than 9 hours to produce such high tilt value starting from a nearly circular/radial shape. Since there are no evidences



vskip 0.3cm

**Fig. 1.** One of the first spokes detected by VIMS in July, 2008. The spoke is faintly observable near the center of this contrast-enhanced image at  $2.23 \mu\text{m}$ .

until now of such long-lived spokes, it is likely that this spoke had a tilted aspect since its birth. Finally, it is darker than the surrounding lit face of the B ring by less than 10% but it is not spatially homogeneous and its densest part lies very near its outer edge, less than 4000 km from the synchronous radius (as defined in the System III reference frame).

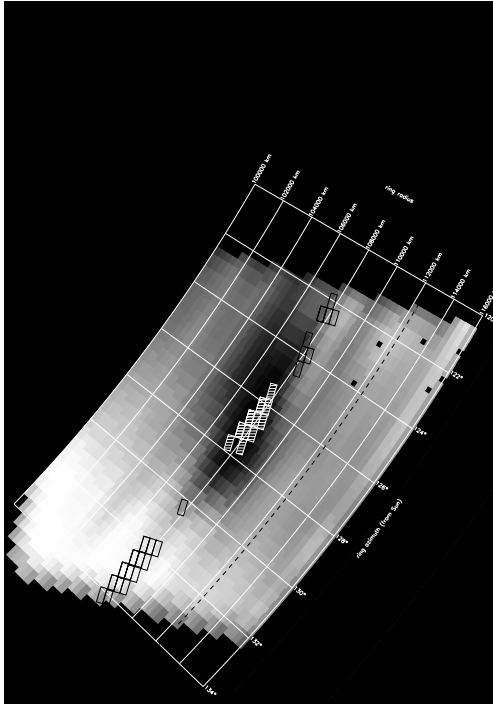


**Fig. 2.** The same image as in Fig.1 projected onto the ring plane. The spoke is very enhanced after azimuthal reflectance normalization ( $\lambda=2.23 \mu\text{m}$ ).

### 3.1. The spatial analysis

The retrieval of the spectral properties of the spoke from the ring data is not trivial, mainly because of the remarkable fine structure typical of the B ring. The influence of the spoke on the ring spectrum can be meaningfully measured only comparing ring spectra inside and outside the spoke but lying exactly on the same ringlet, within the actual spatial resolution of the data. This is needed to avoid the interpretation of the usual variability of the underlying ringlets' structure as a spectral spoke peculiarity. Furthermore, an azimuthal, wavelength-dependent, nearly-linear reflectance trend is detectable in all the ringlets in the spoke images. In order to obtain unbiased spoke spectra, we need to remove this effect, whatever causes it. A linear interpolation of the ringlets' reflectance on both sides of the spoke is sufficient to cancel it out. Since the spoke is a quite faint feature, we have to increase the signal to noise ratio for the spectra by selecting the spoke pixels with the highest contrast, and it is therefore useful to map the spoke contrast overall the image. This can be done by applying to the original image a window-average algorithm, in which the reflectance in a generic pixel  $(i,j)$  is divided by the average reflectance of all the pixels at the same radius  $R$  (within the observative uncertainty  $\Delta R$ ) but with different azimuth  $\phi$  (i.e. outside an azimuthal window of a given width  $w$ ). Analytically, this map can be defined as:

$$M_{ij}(w) = 1 - r_{ij} / \langle r_k \rangle \quad (1)$$

where the  $k$  index is such that

$$|R_k - R_{ij}| \leq \Delta R_{ij} \quad (2)$$

$$|\phi_k - \phi_{ij}| \geq w \quad (3)$$

For  $w=1^\circ$  we can obtain spoke maps like that reported in Fig.3 ( $\lambda=2.23 \mu\text{m}$ ). These maps allow to select the spectra of the densest part of the spoke and to obtain a more reliable spoke spectrum after averaging. The location of the spectra, discussed in the following sections, are shown in fig.2 in details.

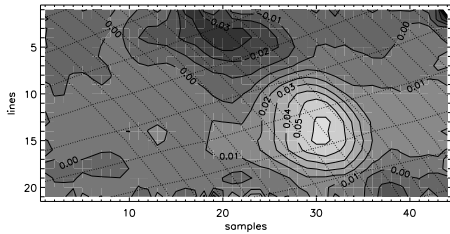


**Fig. 3.** Spoke map obtained from the original reflectance image after window-averaging, as described in text.

### 3.2. The spectral analysis

After the selection process described in the previous sections, we obtain average spectra of the rings inside and outside the bulk of the spoke. The corresponding average spectra are shown Fig.4.

Both spectra are dominated by the water ice absorption bands (broad bands at 1.5, 2.0, 3.0  $\mu\text{m}$  and shallow bands at 1.05 and 1.25  $\mu\text{m}$ ). Only the 2.0  $\mu\text{m}$  band shows a little change, slightly shallower inside the spoke. On the contrary, the Fresnel peak at 3.1  $\mu\text{m}$  and the 4  $\mu\text{m}$  region seem to be totally unaffected by the presence of the spoke. The continuum level inside the spoke appears lower than the reference spectrum everywhere shortward of about 3  $\mu\text{m}$ .

As pointed out by McGhee et al., (2005), the most meaningful quantity to measure the effect of the spoke on the ring reflectance is the spectral contrast  $C = 1 - r_{spk}/r_{ring}$ , since it equals the spoke's optical thickness if it is optically thin. This is true, however, only in a non-scattering approximation of the radiative transfer inside the spoke. By its definition,  $C$  is a positive quantity for a dark spoke. The average spectral contrast of the spoke under study is reported in Fig.5. The spectrum is not shown longward of 2.75  $\mu\text{m}$ , since the high water ice absorption there makes it very noisy.

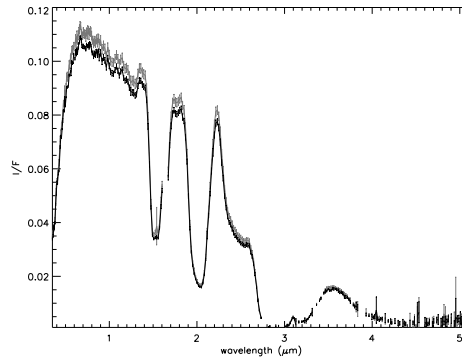


**Fig. 4.** Average VIMS spectra inside (gray) and outside (black) the spoke, as obtained from the pixels indicated in Fig.2

The spoke spectrum shows small decreases of the depths of the main water ice bands, at 1.5  $\mu\text{m}$ , 2.0  $\mu\text{m}$  and 3  $\mu\text{m}$ , together with a rapid increase of contrast in the blue, from 0.35 to 0.60  $\mu\text{m}$ . However, the most interesting feature is that the spoke has a high contrast everywhere in the 1-3  $\mu\text{m}$  range, of the same order or higher than at visible wavelengths. As discussed in D'Aversa et al., (2010), this was not expected on the basis of previous observations, limited to the VIS range, and requires the spoke to have a consistent population of micron-sized particles.

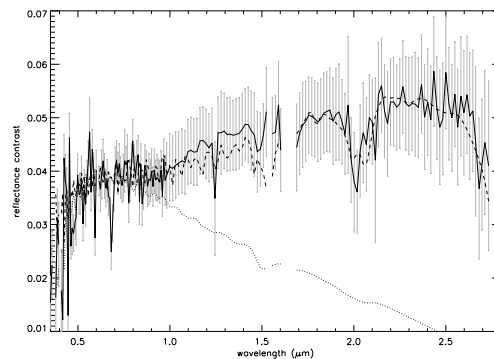


**Fig. 5.** Average spectral contrast of the spoke (solid curve), with 1- $\sigma$  error bars. The dashed line is the best fit to the 0.35-2.75  $\mu\text{m}$  range, while the dotted line refers to the VIS portion only.

### 3.3. The modeling

In order to quantitatively retrieve the size distribution of the spoke's grains responsible for the unexpectedly high infrared contrast, we have to model the spoke and the radiative transfer inside it. We are interested in directly fit the spoke contrast spectrum, while the complete modeling of the unperturbed ring spectra is beyond the purpose of the present work. Therefore we assume the minimum set of hypotheses needed to this purpose: the spoke, overlying the optically unperturbed B ring, consists of a thin uniform sheet of pure water ice particles, homogeneous, spheroidal in shape. The refraction index typical of low-temperature water ice is assumed, as obtained by mixing optical constants from different sources (Bertie et al., 1969; Toon et al., 1994; Warren, 1984; Grundy and Schmitt, 1998).

With these assumptions the simplest model able to reproduce most of the spoke spectral features requires at least three terms:

$$C = 1 - e^{-\tau'} + \frac{D_1}{r_{ring}} + \frac{D_2}{r_{ring}} \quad (4)$$

The first order term  $1 - e^{-\tau'}$  quantifies the extinction of the radiation going through the spoke in the actual geometry. The second- and third-order terms  $D_1$  and  $D_2$  represent the contributions to the outgoing radiation due, respectively, to single and double scattering by spoke particles. These terms are essentially in reproducing the water ice band depths and the blue slope in the contrast spectrum. All these quantities only depend on the spoke number density and on the single scattering parameters of the spoke grains, averaged over a size distribution. Among the several kinds of distribution function that we tested (rectangular, power law, gamma, log-normal, bimodal, etc.), the best fit has been achieved with a log-normal function, shown in Fig.6, extending from about 0.25 to 14  $\mu\text{m}$ , with a modal radius of about 1.9  $\mu\text{m}$ . The resulting model is shown in fig.5.

As conjectured above, this distribution is much wider than previously thought on the basis of visible-only observations. The effective parameters are  $r_{eff}=3.5 \mu\text{m}$  as radius and  $v_{eff}=0.3$  as variance. The model allows also an

estimation of the column density of the spoke ( $14600 \pm 6500 \text{ cm}^{-2}$ ) which is relative to the actual observational geometry. If the spoke sheet is 1-km thick, the resulting number density is  $10^{-1} \div 10^{-2} \text{ cm}^{-3}$ .

If we limit our analysis only to the VIS spectral range, 0.35-1.0  $\mu\text{m}$ , a narrower distribution of water ice grains is sufficient to achieve a good fit to the spectral contrast (Fig.6). In this case we obtain a modal radius of about 0.65  $\mu\text{m}$ , with a column density of about  $(60 \pm 5) \cdot 10^3 \text{ cm}^{-2}$  and the data cannot discriminate between gamma and log-normal distribution functions, which give very similar synthetic spectra. These results are more similar to those inferred by the Voyager and HST observations. However, as can be seen in fig.5, if extrapolated to the infrared range, this populations cannot reproduce the observed level of contrast.

## 4. Discussion

Several constraints to the spoke grain sizes have been established since the spoke discovery, based on observed physical properties or on theoretical considerations. A lower limit of grain size of the order of 0.1  $\mu\text{m}$  has been derived from the observed deviations from keplerian velocities (Thomsen et al., 1982). Important theoretical limits have been inferred from grains stability criteria against electrostatic and centrifugal disruption, suggesting the grains radii to be inside the range of 0.5-3  $\mu\text{m}$  (Thomsen et al., 1982; Meyer-Vernet, 1984). The distribution of grain size inferred from VIMS data, although clearly wider than previous ones, does not contradict these theoretical constraints. It indicates, however, that the spoke can be a more energetic phenomenon than previously thought. In fact, if more than 90% of spoke particles have a radius smaller than the predicted disruption limit, the total mass of the spoke increases at least by two order of magnitude. As a consequence, the charging process needed to trigger the levitation should be more effective at least by one order of magnitude. It is worth noting, however, that our assumptions about the spoke may be not completely reliable. In fact, the forces gov-

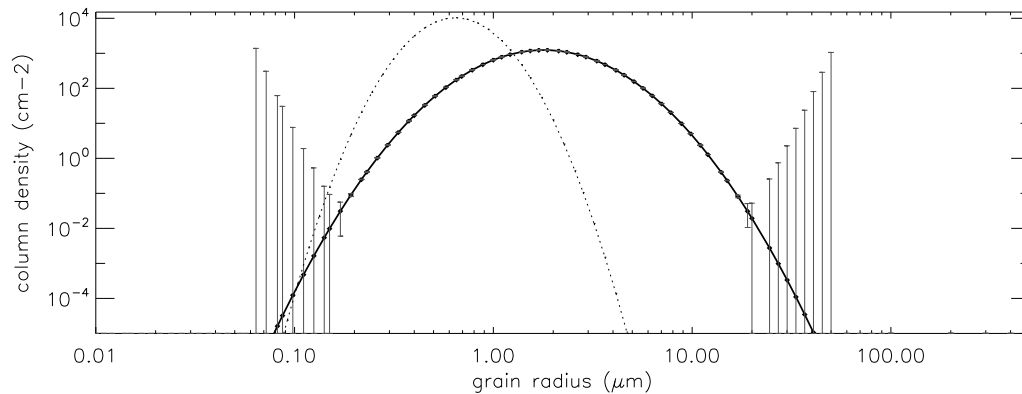


**Fig. 6.** Grain size distribution used to fit the spoke spectrum in the VIMS spectral range 0.35-2.75 $\mu\text{m}$  (solid line). The dotted line indicates the distribution that can fit the visible range only. Formal errors due to the model sensitivity are shown as error bars.

erning the spoke formation and evolution are quite sensitive to the grain size and mass, and are therefore expected to produce significant size selection effects inside the spoke. Our size distribution is instead inferred for a spatially homogeneous spoke, and the effect of a vertical stratification of the grain sizes is not taken into account.

Further analyses are of course needed to confirm or not these preliminary conclusions. Many other spokes have been imaged by VIMS during Saturn equinox, with different geometries and resolutions. They will allow a more statistically meaningful analysis of the retrieved size distributions, and the refinement of the models for the spokes and for their radiative processes.

*Acknowledgements.* This work was supported by ASI, Agenzia Spaziale Italiana.

## References

- Acton, C. H., 1996, *Planet.Space Sci.*, 23, 65  
 Bertie, J. E. et al., 1969, *J.Chem.Phys.*, 50, 4501  
 Brown, R. H. et al., 2004, *Space Sci. Rev.*, 115, 111  
 D'Aversa, E., et al., 2010, *Geophys. Res. Lett.*, 37, L01203, doi:10.1029/2009GL041427  
 Farmer, A. J. & P. Goldreich, 2005, *Icarus*, 179, 535  
 Goertz, C. K. and G. Morfill, 1983, *Icarus*, 53, 219  
 Grundy, W. M. and B. Schmitt, 1998, *J.Geophys.Res.*, 103(E11), 25809  
 Jones, G. H. et al., 2006, *Geophys.Res.Lett.*, 33, L21202, doi:1029/2006GL028146  
 McCord, T.B. et al., 2004, *Icarus*, 172, 104  
 McGhee, C. A., et al., 2005, *Icarus*, 173, 508  
 Meyer-Vernet, N., 1984, *Icarus*, 57, 422  
 Mitchell, C. J., et al., 2006, *Science*, 311, 1587  
 Morfill, G. E. & H. M. Thomas, 2005, *Icarus*, 179, 539  
 Smith, B. A., et al., 1982, *Science*, 215, 504  
 Thomsen, M. F., et al., (1982, *Geophys. Res. Lett.*, 9, 423, (1982, *Geophys. Res. Lett.*, 9, 423  
 Toon, O. B. et al., 1994, *Geophys. Res. Lett.*, 99, 25631  
 Warren, S. G., 1984, *Appl.Opt.*, 23, 1206